IEEE Photonics Journal
An IEEE Photonics Society Publication

Open Access

Sharp Multiple-Phase Resonances in a Plasmonic Compound Grating With Multislits

Volume 10, Number 4, August 2018

Zhimin Liu
Enduo Gao
Fengqi Zhou

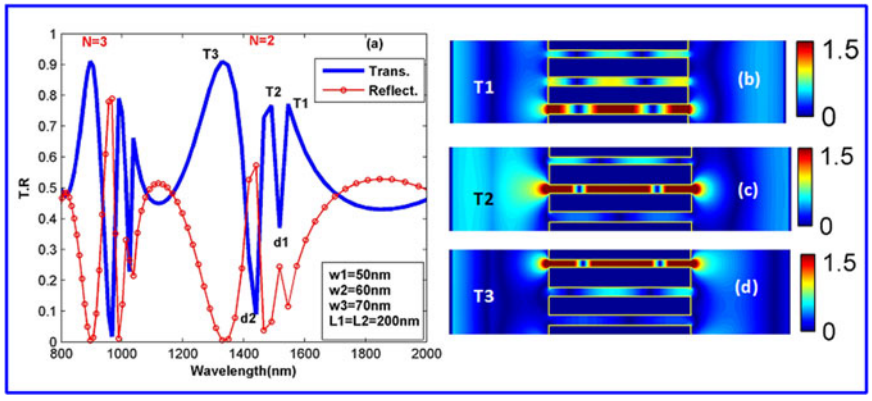

DOI: 10.1109/JPHOT.2018.2844787
1943-0655 © 2018 IEEE

IEEE photonics SOCIETY

IEEE

Sharp Multiple-Phase Resonances in a Plasmonic Compound Grating With Multislits

Zhimin Liu,[1,2] **Enduo Gao**,[1] **and Fengqi Zhou**[1,3]

[1]School of Science, East China Jiaotong University, Nanchang 330013, China
[2]Department of Materials Science and Engineering, The Ohio State University, Columbus, OH 43210 USA
[3]Department of Biomedical Informatics, The Ohio State University, Columbus, OH 43210 USA

DOI:10.1109/JPHOT.2018.2844787

Manuscript received May 17, 2018; accepted June 3, 2018. Date of publication June 8, 2018; date of current version June 21, 2018. This work was supported in part by the National Natural Science Foundation of China under Grant 11164007, in part by the Scientific Project of Jiangxi Education Department of China under Grant GJJ160532, and in part by the Graduate Education Reform Project of Jiangxi Province of China under Grant JXYJG-2017-080, in part by the hundred people long voyage project of Jiangxi Province of China (No. 2017-91), and in part by the visiting scholar project for young teachers' development of Jiangxi general undergraduate Universities (No. 2016-109). Corresponding author: Zhimin Liu (e-mail: liuzhimin2006@163.com).

Abstract: Transmission properties of light through a plasmonic grating with multislits are investigated. The results show that sharp phase resonance (PR) and multiphase resonance (MPR) for each mode at multiple frequencies are achieved and effectively tailored only by adjusting the slight difference of the multislit widths; the values of the PR dips are almost zero. Based on the field distributions, Fabry–Pérot-resonant and phase-resonant mechanisms have been suggested for the physical origins of the observations qualitatively. In addition, we can realize the control of light spreading through an arbitrary slit; a multichannel selector is modeled and described. Compared with the conventional plasmonic compound grating, this multislit grating with different slit widths has obvious advantages, such as simple structure, single material composition, and better realizability. PR and MPR can be achieved at multiple frequencies.

Index Terms: Plasmon resonance, phase resonance, compound grating, multi-phase-resonant.

1. Introduction

It is well known that different kinds of plasmon resonances can be found in a nano-structure system. For example, surface plasmon polariton excitations (SPP) [1]–[3], surface shape resonances (SSR) [4], phase resonances (PR) [5]–[7] and Fano resonances(FR) [8] are reported in metallic grating and nano-particles structures. Recently, multiple plasmon resonances in a nanochannel [9], double FR in coupled plasmonic resonator system [10], multiple FR based on different waveguide modes in a symmetry breaking plasmonic system [11], in optical metamaterials [12] and coupled plasmonic resonator system [13] have also attracted attention and been reported, and the existence of multiple electromagnetically induced transparencies (EIT)-like spectral responses are demonstrated in graphene metamaterials consisting of a series of self-assembled graphene Fabry-Perot

(FP) cavities [14]. The results show that the properties of multiple resonances can be found wide applications in sensors, nonlinear and slow-light devices.

In addition, much attention has been paid to PR in compound metallic grating; the dips of PR often appear in the transmission peaks when the fields are anti-phase distributed, which result from phase difference and destructive interference between adjacent slits or structures. The phase resonances promise the potential applications such as selecting output channel and optical switching [7], tunable antennas, multiwavelength filters and highly sensitive chemical and biological sensors [15], etc. Many methods are used to construct compound structure in order to achieve the phase resonances. Firstly, most authors design the compound metallic nano-structures from the perspective of different structural parameters. For example, symmetrical cut [16] and asymmetrical cut [5], bar [17], bumps [7], semicircle bumps [18], relief slit arrays [19] are proposed. The results of the above papers show that the influence of cuts, bars and bumps in the slit on odd and even modes are different, which lead to changes of the slits' effective length and phase difference, so that the dips in transmission spectrum (namely the phase resonances) will arise. Another way to achieve compound metallic nano-structures is to adjust the dielectric environment, and the transmission behaviors can be effectively tailored by filling different dielectric medium in the slits and holes [20]–[22].

However, multiple phase resonances have been given little consideration up to now. Generally speaking, complex structures of nano-holes and gratings can display novel features, but complex structures cannot be easily constructed and achieved in experiment and device design. The more complex the structures, the harder to design, scan, analyze and work with. Therefore, we want to achieve novel and tunable properties by designing simple and easily realizable structures. In this paper, we investigate phase resonance and Multi-phase-resonant properties in simple and realizable Multi-slits bare gratings with different widths. We found that sharp Multi-phase-resonance-dips for each mode in the transmission spectrum are observed and can be effectively tailored only by adjusting the slight difference of the multi-slits' width. In addition, we can realize a flexible control of light spreading through arbitrary slits of the grating; a multi-channel selector is modeled and described based on the field distributions, F-P and phase resonant mechanisms.

2. Model and Method

A unit cell of a compound metallic grating with three slits (slit 1, 2, 3) is shown in Fig. 1. Fig. 1(a) is a 3-D structure diagram, and Fig. 1(b) is a two-dimensional structure. The length of the grating and period are fixed $h = 1000$ nm and $p = 600$ nm in the whole paper, the reason why we choose the thickness of slit (1 μm) is that we want to discuss the situation of multiple frequencies. It is well known that the larger the slit length compared with the grating period and slit width, the more modes. The widths of slits 1, 2, 3 are tunable denoted by w_1, w_2, w_3, respectively. Slit 2 is located in the central position of the grating; the distances between slit 1 and slit 2, slit 3 and slit 2 are adjustable denoted by L_1, L_2, respectively.

For simplicity, the dielectric spacer and the substrate are not taken into account; i.e., they are treated as air, which does not affect the essential feature except for blueshift or redshift and does not lead to any loss of generality in the discussion that follows. The white areas inside the slits are also air, and magenta areas represent metal, respectively, and the metal is chosen to be gold (Au). The optical properties of the gold nanostructure are approximated by the Drude model and the dispersive permittivity of the frequency is defined as

$$\varepsilon(\omega) = 1 - \frac{\omega_p^2}{\omega^2 + \gamma_p^2} + i\frac{\omega_p^2 \gamma_p^2}{\omega(\omega^2 + \gamma_p^2)} \tag{1}$$

Where ω is the frequency of the incident light, $\omega_p = 1.37 \times 10^{16}\text{s}^{-1}$ and $\gamma_p = 4.08 \times 10^{13}\text{s}^{-1}$ represent the bulk plasmon frequency and the damping rate which characterizes the absorption loss [23].

The structure's response has been investigated using two-dimensional finite-difference time domain (FDTD) [24], [25] with the Meep, Meep is a free and open-source software package for

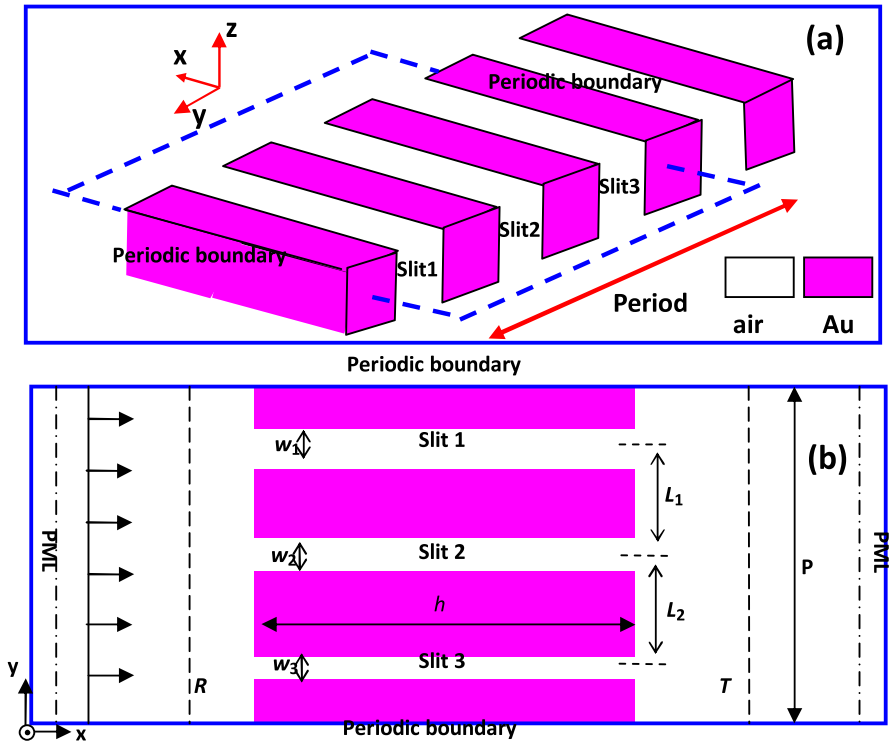

Fig. 1. Scheme of a unit cell of the metallic grating with three slits. (a) A 3-D structure diagram. (b) A two-dimensional structure.

simulating electromagnetic systems via the FDTD method, and is an acronym for MIT Electromagnetic Equation Propagation. The boundaries on the top and bottom of the unit cell in Fig. 1(b) are truncated by periodic boundary conditions (PBC); the boundaries along the *x* direction are treated by perfectly matched layer. The incident light transmits from the left side of the grating, and spreads through the x direction, which is located 400 nm away from the front of surface. The probe location of transmission spectra is set at 400 nm away from the rear surface of the export, and the probe location of reflection spectra is set at 280 nm away from the front of the grating's surface. The calculated spectra are normalized by the calculation without a metallic structure. Specifically, we calculate the results without a metallic structure firstly, and then the results with a metallic structure are calculated. The probe locations of transmission and reflection spectra are the same. Finally, we get the normalized results by comparing the results of the second calculation with the first calculation. And the absorption spectra are obtained by $A = 1 - T - R$, where T, R, and A represent the transmittance, reflectance, and absorbance, respectively.

3. Results and Discussion

3.1 Symmetric Slit

Firstly, we discuss the case of $w_1 = w_2 = w_3 = 50$ nm in order to better understand the transmission property, this means that the three slits' width of the grating are the same. Slit 2 is located in the central position of the grating, and the distances between slit 1, 3 and slit 2 are $L_1 = L_2 = 200$ nm. Therefore, the fields in all slits are equal taking into account the PBC mentioned earlier when light is incident normally. So the structure is equal to a unit cell of a grating with one slit, just like as the scheme shown in Fig. 2(b), the length, slit width and period of the grating are $h = 1000$ nm, $w = 50$ nm, and $p = 200$ nm, respectively. We calculate the transmission, reflection, and absorption spectra, which are shown in Fig. 2(a). The results in Fig. 2 (blue line) shows that the

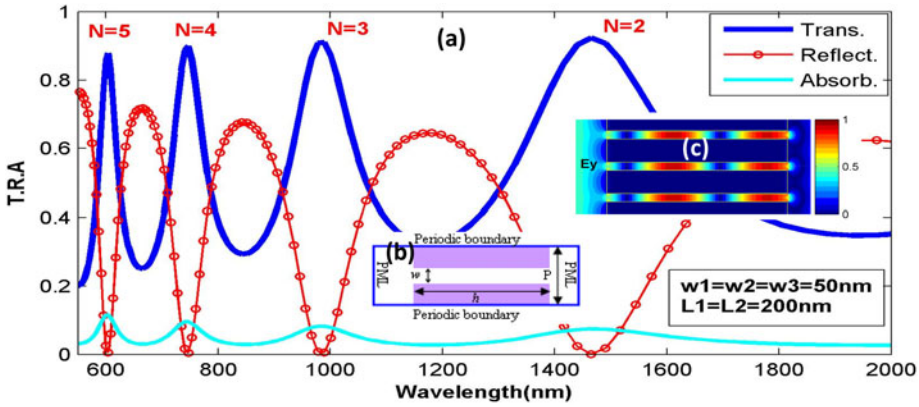

Fig. 2. (a) A Transmission, reflection, and absorption spectra for the three slits with same structural constants. (b) A unit cell of a metallic grating with one slit. (c) The magnitudes of electric field $|E_y|$ for mode N = 2 (λ_1 = 1465 nm, which are labeled in Fig. 3(b)).

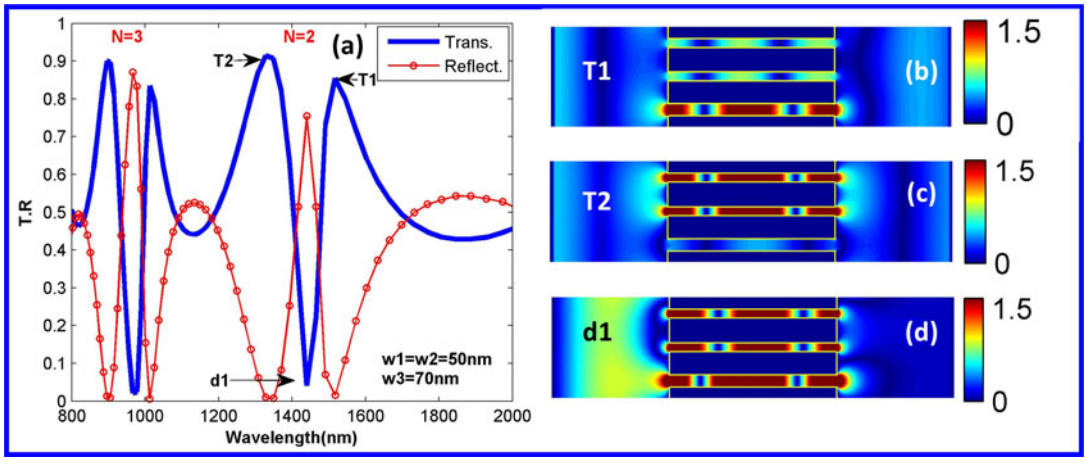

Fig. 3. (a) Transmission and reflection spectra as a function of wavelength for different slit width. (b)–(d) The magnitudes of electric field $|E_y|$ for different wavelength of T1 ($\lambda_1 = 1517$ nm), T2($\lambda_2 = 1328$ nm), d1($\lambda_3 = 1440$ nm), which are labeled in Fig. 3(a).

Fabry–Pérot–like modes resonant peaks appeared at 1465 nm, 989 nm, 747 nm and 604 nm, according to previously reported results [7], [26], which are labeled N = 2, N = 3, N = 4 and N = 5, respectively. Fig. 2(c) show the electric field with two nodes and antinodes for the resonant peak N = 2.

3.2 Asymmetric Slit

Next, the results of the metallic gratings with different slit widths or separation distances are discussed. This means that the structure is asymmetrical; we call it a compound grating.

3.2.1 The Case of $w_1 = w_2 \neq w_3$, Which Means that the Width of Two Slits Is the Same and Is Different From the Width of the Third Slit: Firstly, we fixed $L_1 = L_2 = 200$ nm and set $w_1 = w_2 = 50$ nm, $w_3 = 70$ nm, respectively, which means that the width of two slits is the same and is different from the width of the third slit. The transmission(blue line), reflection(red circle line) spectrums and field distributions are shown in Fig. 3(a)–(d). In order to express this more clearly, only the resonant modes of N = 2 and N = 3 are shown in Fig. 3(a), and the wavelength of the spectrum ranges from 800 nm to 2000 nm. The result shows that almost all of the waveguide resonance peaks exhibit sharp dips. Taking mode N = 2 as an example, two transmission peaks (T1 and T2) are located on

the sides of the dip (d1), and all of the values of the dips are almost equal to zero. The red circle line in Fig. 3(a) shows that there are strong reflections at the transmission dips, in other words, if this is a transmission dip, light cannot be transmitted, and naturally it shows a strong reflection. These phenomena can be seen more clearly from the field distributions in later paragraphs. We attribute this phenomenon of resonant dips to the phase resonance, which arose from the phase difference at the slits' exits. The physical origin can be explained in terms of phase resonances as follows.

We know that the condition of the F-P can be expressed as $k_0 \mathrm{Re}(n_{eff}) L_{FP} + \arg(\rho) = n\pi$ [7], which are characterized by constructive interference between all transmitted waves along the slit, so we found that the transmission properties can be adjusted not only by altering L_{FP}, but also by the effective refractive index n_{eff} in the slit. The effective refractive index n_{eff} depends on the slit width strongly, which can be obtained by solving the dispersion equation [27]:

$$\varepsilon_m \sqrt{n^2_{eff} - \varepsilon_d} \tanh\left(\frac{w\pi\sqrt{n^2_{eff} - \varepsilon_d}}{\lambda}\right) + \varepsilon_d \sqrt{n^2_{eff} - \varepsilon_m} = 0 \tag{2}$$

Where w is the width of slit or waveguide, ε_d and ε_m are permittivities for the dielectric and metal, respectively. For sufficiently small gap widths ($w \to 0$), one can use the approximation $\tanh x \asymp x$. The solution of the equation (2) is

$$n^2_{eff} = \varepsilon_d + \frac{1}{2}\left(\frac{k^{(0)}_{\mathrm{MDM}}}{k_0}\right)^2 + \sqrt{\left(\frac{k^{(0)}_{\mathrm{MDM}}}{k_0}\right)^2 [\varepsilon_d - \varepsilon_m] + \frac{1}{4}\left(\frac{k^{(0)}_{\mathrm{MDM}}}{k_0}\right)^2} \tag{3}$$

Where $k^{(0)}_{MDM} = -2\varepsilon_d / w\varepsilon_m$ represents the wave vector in free space and MDM waveguide ($w \to 0$). Considering different gap-width-dependent terms in Eq. (3), one notices that for not too small gaps, i.e., when $|k^{(0)}_{MDM}| < k_0 \Leftrightarrow w > \frac{\lambda\varepsilon_d}{\pi|\varepsilon_m|}$, $(\frac{k^{(0)}_{\mathrm{MDM}}}{k_0})^2 \to 0$, it can be approximated as follows:

$$n_{eff} = \frac{k_{MDM}}{k_0} \approx \sqrt{\varepsilon_d - \frac{2\varepsilon_d\sqrt{\varepsilon_d - \varepsilon_m}}{k_0 w \varepsilon_m}} \tag{4}$$

Where $k_0 = 2\pi/\lambda$ and k_{MDM} are the wave vectors in free space and MDM waveguide.

If the slits are set symmetrically including width and position, the translation invariance can reduce the field degrees of freedom to just like a single slit array. Therefore, the fields in all slits are equal when the light is normal incidence. While if the slits' width are different, the fields inside the slits are not identical, which shows that there exists a phase difference, and it is also understandable that the field's phases in the slits are unequal [6], [7]. When the phase difference between adjacent slits reached a certain value, an obvious dip resulted from destructive interference between adjacent slits.

Now, let us make a comparison between the above results and previously reported paper [7]. We introduced perpendicular bumps and cuts into the slits previously, and found that bumps and cuts only affect one or several modes. Furthermore when the bumps or cuts are located at the center of antinodes, which have the most influence on the modes and the effective length of the F-P cavity. However, the bumps or cuts are not located at the center of the antinodes, which influence modes slightly. In contrast, slit width impacts all modes, so we see that all peaks of modes exhibit dips. The obvious advantage of this method to achieve phase resonance is simple and easily realizable.

In order to understand the dependence of phase resonance on slit's width well, we draw the distributions of electric field $|E_y|$ for different wavelengths of T1 ($\lambda_1 = 1517$ nm), T2($\lambda_2 = 1328$ nm), d1($\lambda_3 = 1440$ nm), in Fig. 3(b)–(d), which are labeled in Fig. 3(a). It is more meaningful that the electric field $|E_y|$ for the peak T1 at the longer wavelength of the dip d1 is mainly concentrated on the bottom slit, which is shown in Fig. 3(b). While for the peak T2 at the shorter wavelength of the dip d1, the electric field $|E_y|$ distributes mainly in the upper two slits, which is shown in Fig. 3(c). Although the electric field $|E_y|$ for transmission dip (d1) is propagated into the three slits, the wave cannot propagate over the slits, which shows properties of strong reflection. The strong light field distribution can be seen on the left side of the grating. We consider that the above phenomenon

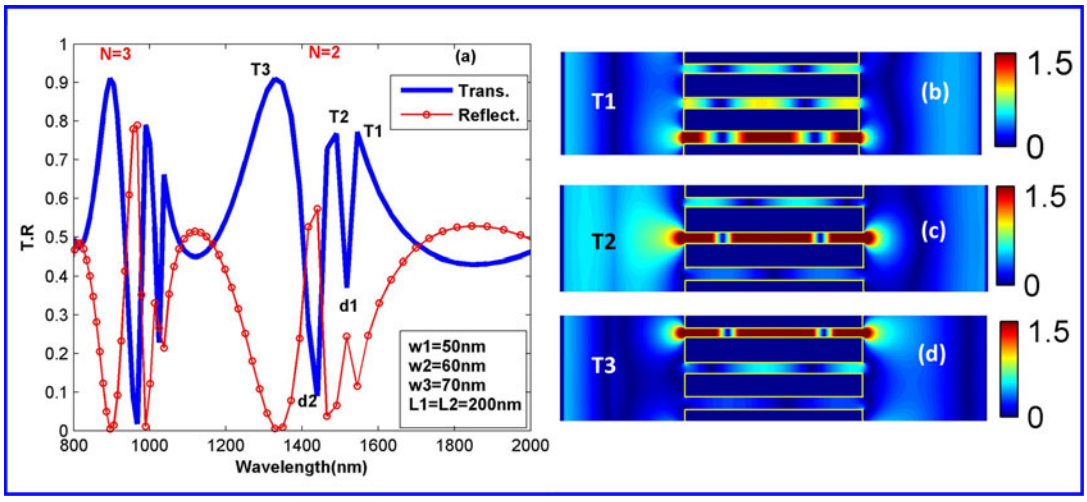

Fig. 4. (a) Transmission and reflection spectra as a function of wavelength for different width of three slits. (b)–(d) The magnitudes of electric field $|E_x|$ for different wavelength of T1, T2, T3, which are labeled in Fig. 3(a).

is attributed to destructive interference of phase difference between slits. This phenomenon also occurs on the other peaks of resonant modes (not shown here).

3.2.2 The Case of $w_1 \neq w_2 \neq w_3$*:* In the above Section 3.2.1, we show that the dips in transmission spectrum and the phase resonance can be tuned by changing the slit's width. When the widths of three slit are different, that is $w_1 \neq w_2 \neq w_3$, can the phase resonance be achieved, and will new phenomenon happen?

Secondly, In Fig. 4 (a)–(d), we plot the transmission (blue line), reflection (red circle line) spectrums and field distributions of Multi-slit gratings with different slit width, the widths of slit 1, 2, 3 are set $w_1 = 50$ nm,$w_2 = 60$ nm, $w_3 = 70$ nm, respectively, and the distances between slit 1, 3 and slit 2 are fixed $L_1 = L_2 = 200$ nm. As above, only N = 2 and N = 3 resonant modes in the spectrum of the wavelength ranges from 800 nm to 2000 nm are presented in order to show more clearly. We find that almost all the waveguide resonance peaks exhibit sharp dips in the transmission spectrum. It is amazing that there are two sharp dips in each mode, and three transmission peaks (T1, T2 and T3) are located on the sides of the dips (d1 and d2). This phenomenon can be considered to be multiple phase resonance (MPR). Why? Based on the previous analysis, the effective refractive index n_{eff} strongly depends on the slit width. Given that the widths of the three slits are unequal, the effective refractive index n_{eff} of the three slits are different, it is also understandable that the propagated phases and fields of the three slits are dissimilar [5], [6], [7], which leads to twice phase difference for the three slits. When the phase difference between adjacent slits reaches a certain value, which will lead to twice the destructive interference between the three slits, then two obvious dips appear. In accordance with the above results, we can infer that two and three dips can be realized by twice and thrice destructive interference, and so on.

What is the significance and advantage of multiple phase resonance? We also draw the electronic field distributions in Fig. 4(b)–(d) for three transmission peaks (T1, T2 and T3). The wavelengths of three transmission peaks (T1, T2 and T3) are $\lambda = 1545$ nm (T1), $\lambda = 1491$ nm (T2) and $\lambda = 1328$ nm (T3), which are labeled in Fig. 4(a). It is interesting that the electric field $|E_y|$ of resonant peak (T1) is most concentrated on the bottom slit with width $w_3 = 70$ nm, and the electric field $|E_y|$ of the resonant peak (T2) is determined by the middle slit with width $w_2 = 60$ nm, then the electric field $|E_y|$ of the resonant peak (T3) is mainly focused on the top slit with width $w_1 = 50$ nm. The results confirm that the interference behavior of phase resonances between adjacent slits are able to be modulated by arranging different slit's width, which may bring many new applications. For example, this structure and method of adjusting transmission spectra and fields can be proposed

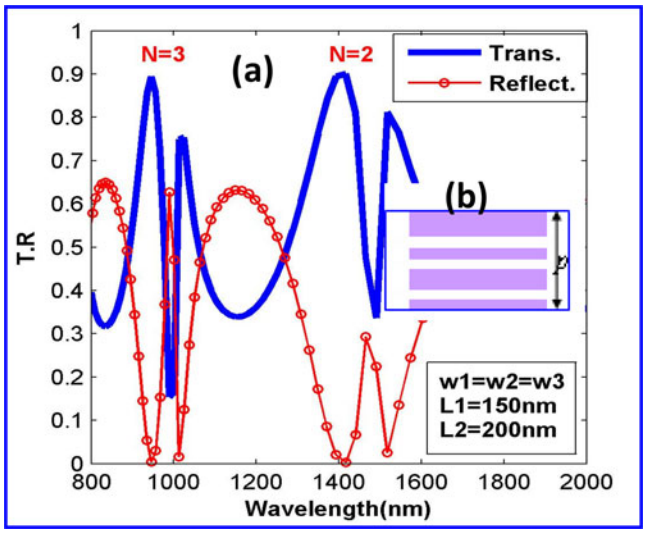

Fig. 5. (a) Transmission and reflection spectra as a function of wavelength for different vertical displacements $L_1 = 150$ nm, $L_2 = 200$ nm between the top, bottom and middle slit. (b) Scheme of a unit cell of a metallic grating.

as a new method to achieve channel selecting devices, new types of actively-controlled nano-optic devices, frequency selector or filter, and optical switching, etc.

3.2.3 The Case of L1 ≠ L2, Which Means Vertical Displacements Between Top, Bottom and Middle Slit Are Different: In the above Sections 3.2.1 and 3.2.2**,** we show that the phase resonance can be achieved and adjusted by varying the slit width, but vertical spacing distances between the top, bottom and middle slit are always kept the same. Can phase resonance be achieved only by varying vertical spacing distances between the top, bottom and middle slit for the same slit width?

Fig. 5 shows the transmission(blue line), reflection(red circle line) spectrums of Multi-slit grating with different vertical spacing distances $L_1 = 150$ nm, $L_2 = 200$ nm between the top, bottom and middle slit, the slit widths are fixed $w_1 = w_2 = w_3 = 50$ nm. It is surprised to find that phase resonances also occur, and similar to previous results, the dips in the transmission spectrum are very sharp. Let's analyze grating the structure again: in Fig. 1, the calculated region along the *y* direction of the unit cell is truncated by PBC, and the grating period is fixed $p = 600$ nm. Although the three slits are completely the same including width and length, when we set different vertical spacing distances $L_1 \neq L_2$, the translation variance cannot reduce the field degrees of freedom to a single periodic slit array, so phase resonance still appears because this structure is seen as compound metallic grating.

Compared with the conventional plasmonic compound grating, this multi-slit grating with different slit widths has obvious advantages, such as simple structure, single material composition, the simplicity and realizability to design, scan, analyze and work with, also the characteristics can be achieved at multiple frequencies.

4. Conclusions

In summary, the transmission properties of light through a plasmonic grating with multi-slits are investigated by using the FDTD method. The tunable phase resonant properties can be achieved by designing a simple and realizable plasmonic grating with different widths of multi-slits. Sharp Multi-phase-resonance-dips for each mode in the transmission spectrum are observed and can be effectively tailored only by adjusting the slight difference of the multi-slits' width. We can realize the control of light spreading through an arbitrary grating slit, and a multi-channel selector is modeled and described. Compared with the conventional plasmonic compound grating, this multi-

slit grating with different slit widths has obvious advantages, such as simple structure, single material composition, better realizability, and PR and MPR can be achieved at multiple frequencies. We expect that our findings are useful and experimental guidance for the design of optical devices, and contribute to more applications in the future.

Acknowledgment

The authors thank Mary Anna Wildermuth for discussions and revision of this paper.

References

[1] T. W. Ebbesen, H. J. Lezec, H. F. Ghaemi, T. Thio, and P. A. Wolff, "Extraordinary optical transmission through sub-wavelength hole arrays," *Nature (London)*, vol. 391, pp. 667–669, Feb. 1998.
[2] H. F. Ghaemi, T. Thio, D. E. Grupp, T. W. Ebbesen, and H. J. Lezec, "Surface plasmons enhance optical transmission through subwavelength holes," *Phys. Rev. B*, vol. 58, pp. 6779–6782, Sep. 1998.
[3] W. L. Barnes, W. A. Murray, J. Dintinger, E. Devaux, and T. W. Ebbesen, "Surface plasmon polaritons and their role in the enhanced transmission of light through periodic arrays of subwavelength holes in a metal film," *Phys. Rev. Lett*, vol. 92, Mar. 2004, Art. no. 107401.
[4] R. A. Depine and D. C. Skigin, "Resonant modes of a bottle shaped cavity and their effects in finite and infinite gratings," *Phys. Rev. E*, vol. 61, pp. 4479–4490, Apr. 2000.
[5] X. Zhai, J. Q. Liu, M. D. He, L. L. Wang, S. C. Wen, and D. Y. Fan, "Adjustable phase resonances in a compound metallic grating with perpendicular cuts," *Opt. Exp.*, vol. 18, no. 7, pp. 6871–6876, Mar. 2010.
[6] Z. Liu and G. Jin, "Resonant acoustic transmission through compound subwavelength hole arrays: The role of phase resonances," *J. Phys: Condens Matter*, vol. 21, Oct. 2009, Art. no. 445401.
[7] Z. M. Liu, H. J. Li, and S. X. Xie, "Tunable phase resonances in a compound metallic grating with perpendicular bumps and cuts," *Opt. Exp.*, vol. 19, no. 5, pp. 4217–4223, Feb. 2011.
[8] V. Gregory, H. Riad, and B. Nathalie, "Nearly perfect fano transmission resonances through nanoslits drilled in a metallic membrane stephane collin," *Phys. Rev. Lett.*, vol. 104, no. 2, pp. 027401–027404, Jan. 2010.
[9] W. Peng, Y. Z. Liang, L. X. Li, Y. Liu, and J. F. Masson, "Generation of multiple plasmon resonances in a nanochannel," *IEEE Photon. J*, vol. 5, no. 4, Aug. 2013, Art. no. 4500509.
[10] H. X. Fu *et al.*, "Independently tunable ultra-sharp double fano resonances in coupled plasmonic resonator system," *IEEE Photon. J*, vol. 10, no. 1, Feb. 2018, Art. no. 4800409, doi: 10.1109/JPHOT.2018.2791612.
[11] Z. Chen and L. Yu, "Multiple fano resonances based on different waveguide modes in a symmetry breaking plasmonic system," *IEEE Photon. J*, vol. 6, no. 6, Dec. 2014, Art. no. 4802208.
[12] Y. T. Moritake, Y. Kanamori, and K. Hane, "Demonstration of sharp multiple Fano resonances in optical metamaterials," *Opt. Exp.*, vol. 24, pp. 9332–9339, May 2016.
[13] S. L. Li, Y. Y. Zhang, X. K. Song, Y. L. Wang, and L. Yu, "Tunable triple Fano resonances based on multimode interference in coupled plasmonic resonator system," *Opt. Exp.*, vol. 24, pp. 15351–15361, May 2016.
[14] C. Zeng, Y. D. Cui, and X. M. Liu, "Tunable multiple phase-coupled plasmon-induced transparencies in graphene metamaterials," *Opt. Exp.*, vol. 23, pp. 545–551, Jan. 2015.
[15] I. M. Mandel, A. B. Golovin, and D. T. Crouse, "Fano phase resonances in multilayer metal-dielectric compound gratings," *Phys. Rev. A*, vol. 87, May 2013, Art. no. 053847.
[16] Y. H. Wang, Y. Q. Wang, Y. Zhang, and S. T. Liu, "Transmission through metallic array slits with perpendicular cuts," *Opt. Exp.*, vol. 17, pp. 5014–5022, Mar. 2009.
[17] M. D. He, Z. Q. Gong, and S. Li, "Light transmission through metallic slit with a bar," *Solid State Commun*, vol. 150, pp. 1283–1286, Aug. 2010.
[18] X. Zhou, J. S. Fang, D. W. Yang, B. Tang, and Z. M. Liu, "Optical transmission through compound gold surface relief slit arrays," *Opt. Exp.*, vol. 22, pp. 1085–1093, Jan. 2014.
[19] X. Zhou, J. S. Fang, Q. Q. Zhu, B. Tang, and Z. M. Liu, "Investigation of optical transmission through a gold grating with semicircle bumps using FDTD method," *Modern Phys. Lett. B*, vol. 27, Jul. 2013, Art. no. 1350126.
[20] X. N. Zhang, G. Q. Liu, and Y. Hu, "Tunable extraordinary optical transmission in a metal film perforated with two-level subwavelength cylindrical holes," *Plasmonics*, vol. 9, pp. 1149–1153, Oct. 2014.
[21] D. Xiang, L. L. Wang, and X. F. Li, "Transmission resonances of compound metallic gratings with two subwavelength slits in each period," *Opt. Exp.*, vol. 19, pp. 2187–2192, Jan. 2011.
[22] Y. Xiao, Z. M. Liu, and F. Q. Zhou, "Effects of dielectric environment on phase resonance in compound grating," *J. Nanomater.*, vol. 2015, Aug. 2015, Art. no. 179621.
[23] A. Taflove and S. C. Hagness, *Computational Electrodynamics: The Finite-Difference Time-Domain Method*. Boston, MA, USA: Artech House, 2000.
[24] K. S. Yee, "Numerical solution of initial boundary value problems involving Maxwell's equations in isotropic media," *IEEE Trans. Antennas Propag.*, vol. 14, no. 3, pp. 302–307, May 1966.
[25] E. D. Palik, *Handbook of Optical Constants in Solids*. Boston, MA, USA: Academic, 1982.
[26] A. P. Hibbins, M. J. Lockyear, and J. R. Sambles, "The resonant electromagnetic fields of an array of metallic slits acting as Fabry-Perot cavities," *J. Appl. Phys*, vol. 99, Mar. 2006, Art. no. 124903.
[27] S. I. Bozhevolnyi and J. Jung, "Scaling for gap plasmon based waveguides," *Opt. Exp.*, vol. 16, pp. 2676–2684, Feb. 2008.